Cell Reports

Article

Transcription factor Ascl2 promotes germinal center B cell responses by directly regulating AID transcription

Graphical abstract

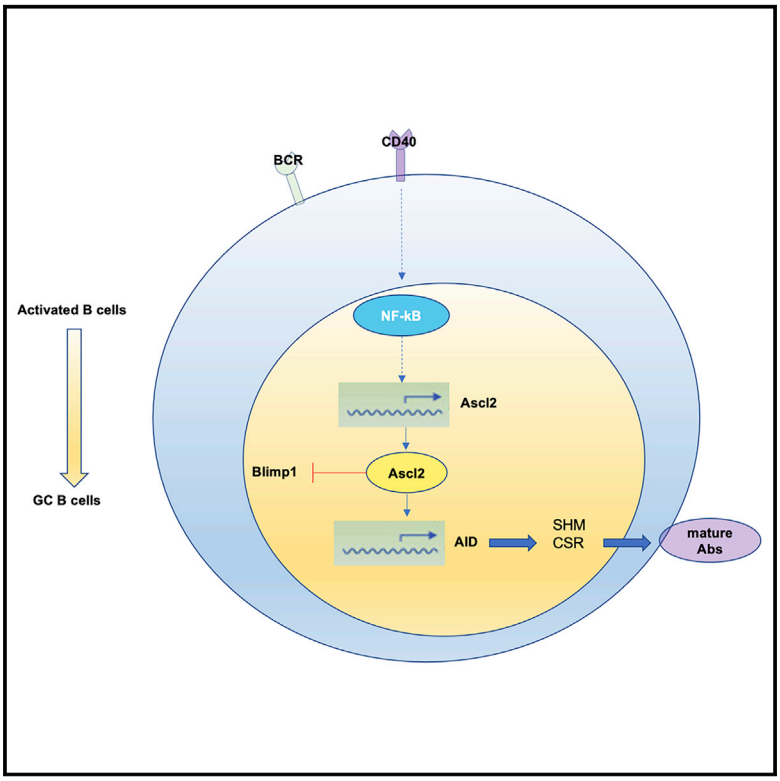

Authors

Lin Sun, Xiaohong Zhao, Xindong Liu, ..., Hui Wang, Xiaohu Wang, Chen Dong

Correspondence

chendong@tsinghua.edu.cn

In brief

Sun et al. find that Ascl2 promotes GC B cell development and enhances antibody production and affinity maturation. Genome-wide analysis reveals that Ascl2 directly regulates GC B cell-related genes, including AID.

Highlights

- *Ascl2* promotes germinal center B cell development and enhances antibody responses
- Deletion of *Ascl2* in B cells impairs the germinal center response
- Genome-wide analysis reveals that Ascl2 directly regulates GC B cell-related genes
- Ectopic expression of AID in *Ascl2*-deficient B cells rescues their antibody defects

Sun et al., 2021, Cell Reports *35*, 109188
June 1, 2021
https://doi.org/10.1016/j.celrep.2021.109188

CellPress

Cell Reports

CellPress
OPEN ACCESS

Article

Transcription factor Ascl2 promotes germinal center B cell responses by directly regulating AID transcription

Lin Sun,[1,2] Xiaohong Zhao,[1] Xindong Liu,[3] Bo Zhong,[4] Hong Tang,[5] Wei Jin,[1] Hans Clevers,[6] Hui Wang,[7] Xiaohu Wang,[1] and Chen Dong[1,8,9,*]

[1]Institute for Immunology and School of Medicine, Tsinghua University, Beijing, China
[2]Tsinghua University-Peking University Joint Center for Life Science, Beijing 100084, China
[3]Institute of Pathology and Southwest Cancer Center, Southwest Hospital, Third Military Medical University, Chongqing, China
[4]State Key Laboratory of Virology, Hubei Key Laboratory of Cell Homeostasis, College of Life Sciences, Wuhan University, Wuhan, China
[5]CAS Key Laboratory of Molecular Virology and Immunology, Institute Pasteur of Shanghai, Chinese Academy of Sciences, Beijing, China
[6]Hubrecht Institute, Royal Netherlands Academy of Arts and Sciences (KNAW) and University Medical Centre (UMC) Utrecht, 3584 CT Utrecht, the Netherlands
[7]Department of Immunology and Center for Inflammation and Cancer, MD Anderson Cancer Center, Houston, TX 77054, USA
[8]Beijing Key Lab for Immunological Research on Chronic Diseases, Beijing 100084, China
[9]Lead contact
*Correspondence: chendong@tsinghua.edu.cn
https://doi.org/10.1016/j.celrep.2021.109188

SUMMARY

During germinal center (GC) reactions, activated B cells undergo clonal expansion and functional maturation to produce high-affinity antibodies and differentiate into plasma and memory cells, accompanied with class-switching recombination (CSR) and somatic hypermutation (SHM). Activation-induced cytidine deaminase (AID) is responsible for both CSR and SHM in GC B cells. Transcriptional mechanisms underlying AID regulation and GC B cell reactions are still not well understood. Here, we show that expression of Ascl2 transcription factor is upregulated in GC B cells. Ectopic expression of *Ascl2* promotes GC B cell development and enhances antibody production and affinity maturation. Conversely, deletion of *Ascl2* in B cells impairs the GC response. Genome-wide analysis reveals that Ascl2 directly regulates GC B cell-related genes, including AID; ectopic expression of AID in *Ascl2*-deficient B cells rescues their antibody defects. Thus, Ascl2 regulates AID transcription and promotes GC B cell responses.

INTRODUCTION

The germinal center (GC), the hallmark of T-dependent humoral immunity, is where antigen-activated B cells proliferate and differentiate into plasma and memory cells. Somatic hypermutation (SHM) and class-switching recombination (CSR) also occur during GC reactions, leading to production of high-affinity and class-switched antibodies. Activation-induced cytidine deaminase (AID), encoded by *Aicda*, is required for both CSR and SHM; *Aicda*-deficient animals and humans display no CSR or SHM in the immunoglobulin (Ig) genes (Cogné, 2013; Muramatsu et al., 2000; Revy et al., 2000). To induce isotype switching, AID has been shown to be recruited to the Ig genes in switch regions immediately 5′ to Cμ and to another heavy-chain constant region (Cogné et al., 1994; Pinaud et al., 2001, 2011; Vincent-Fabert et al., 2010). Indeed, an E-box motif CANNTG increased the mutation of an associated sequence without influencing AID transcription (Yabuki et al., 2009).

Bcl6 is the master transcription factor in control of GC reactions, including GC B cell activation and differentiation (Dent et al., 1997; Ye et al., 1997). Selective ablation of *Bcl6* in B cells impaired GC reactions and production of high-affinity antibodies (Basso and Dalla-Favera, 2012). Besides Bcl6, E proteins, a family of transcription factors that recognize the E-box (CANNTG) motif with similar sequence specificity, are also implicated in GC B cell development. E proteins can be sequestered by the inhibitor of DNA-binding (Id) proteins that lack the basic DNA-binding domain (Murre, 2005). Overexpression of Id3 in B cells prevented the binding of E proteins to the *Aicda* locus, which caused defective *Aicda* transcription, and thus CSR (Sayegh et al., 2003). E2A (with two isoforms, E12 and E47) is regarded as the dominant E protein in B cell lineage commitment and early B cell development. E2A was shown to be dispensable for GC B cell development, as suggested by the conditional *Tcf3* (encoding E2A) inactivation, although it was abundantly expressed in GC centroblasts (Kwon et al., 2008). E2-2, another E protein expressed in B cells, was also suggested to be not important for B cell development and differentiation in early studies (Wikström et al., 2006). However, recent studies suggest that E2A and E2-2 may play an important role in late-stage B cell differentiation and plasma cell development through regulating CSR (Gloury et al., 2016; Wöhner et al., 2016). Despite these studies,

the role of E proteins in GC B cell development, particularly in SHM, is largely unclear.

Our previous work showed that Achaete scute-like 2 (Ascl2), a member of the E protein family, initiates follicular helper T (Tfh) cell development through upregulating the expression of CXCR5 in activated T cells and regulating T cell homing to the follicles (Liu et al., 2014). In this study, we uncover a critical role for Ascl2 in the transcriptional regulation of GC B cell development. Genome-wide analysis revealed that Ascl2 directly regulates AID expression. Thus, in addition to its role in Tfh cells, Ascl2 also promotes GC B cell responses.

RESULTS

Ascl2 is selectively expressed in GC B cells

Considering the important role of Ascl2 in regulating Tfh cell development, it is interesting to know whether Ascl2 also regulates GC B cells. To assess this, we sorted GC B ($IgD^{-}Fas^{+}GL7^{+}$) and activated non-GC B cells ($IgD^{-}Fas^{-}GL7^{-}$) from the Bcl6-RFP reporter mice (Liu et al., 2012) following keyhole limpet hemocyanin (KLH) immunization for further analysis. The expression of Bcl6 was clearly higher in GC B cells versus activated non-GC B cells as determined at mRNA level or via the reporter expression (Figure 1A). Notably, the mRNA for *Ascl2* was dramatically increased in GC B versus activated non-GC B cells (Figure 1B). To evaluate Ascl2 expression in antigen-specific B cells, we transferred naive MD4 B cells into CD45.1 recipient mouse together with naive OT-II T cells, followed by immunization with ovalbumin (OVA)-hen egg lysozyme (HEL) emulsified in complete Freund's adjuvant (CFA). The HEL-specific MD4 GC and activated non-GC B cells were isolated 7 days later for examining the mRNA level of *Ascl2*. Consistent with KLH immunization, the mRNA level of *Ascl2* was markedly higher in GC than in activated non-GC B cells (Figure 1C).

To further validate this result, we generated Ascl2-ZsGreen reporter knockin mice (Figure S1A). After KLH/CFA immunization, Ascl2 reporter expression was selectively detected in GC, but not activated non-GC B cells (Figure 1D). Moreover, the Ascl2 reporter signal was preferentially detected in Tfh than non-Tfh cells (Figure S1B), consistent with Liu et al. (2014) work showing that Ascl2 mRNA expression was much higher in Tfh cells than non-Tfh cells by real-time PCR.

Ascl2 thus appears to be upregulated in GC B cells. To assess the signals regulating Ascl2 upregulation, we isolated naive B ($CD38^{-}IgD^{+}$) cells from the Ascl2 reporter mice and stimulated them *in vitro* with anti-IgM and anti-CD40. Interestingly, Ascl2 was readily increased in activated compared with naive B cells, as examined at mRNA level (Figure 1E) or by Ascl2 reporter expression (Figure 1F). Ascl2 expression could not be induced by anti-IgM alone or further enhanced by cytokines interleukin-4 (IL-4), IL-21, interferon γ (IFN-γ), or transforming growth factor β (TGF-β) in B cell cultured in the presence of both anti-IgM and anti-CD40 (Figure 1H). Moreover, overexpression of Bcl6 could not induce the expression of Ascl2 (Figure 1G). However, anti-CD40 or lipopolysaccharide (LPS) stimulation induced significant expression of Ascl2 (Figure 1H), suggesting a critical role of nuclear factor κB (NF-κB) pathways in the regulation.

Enforced Ascl2 expression promotes GC B cell development

The above expression data suggest that Ascl2 may participate in GC B cell differentiation and development. To examine this, we retrovirally overexpressed Ascl2 in LPS-activated B cells followed by stimulation with anti-IgM and anti-CD40 *in vitro*. Interestingly, total IgG production was increased by ~10-fold and IgA by ~2-fold in Ascl2-transduced B cells than those infected with control virus; IgM appeared to be increased, although it did not reach statistical significance (Figure 2A). Notably, overexpression of Id3 in Ascl2-transduced B cells inhibited Ascl2 function in elevating IgG production *in vitro* (Figure 2A). Similar to our earlier finding in T cells (Liu et al., 2014), Ascl2 overexpression did not induce expression of *Bcl6* or *Prdm1* but drastically increased the expression of *Aicda* (~5-fold increase) (Figure 2B).

To examine whether Ascl2 regulates B cell function *in vivo*, we first infected MD4 B cells with Ascl2-containing or control retrovirus and transferred it into Rag1-deficient mice together with OT-II T cells. The recipient mice were sacrificed and analyzed 7 days following OVA-HEL immunization. As expected, Ascl2 overexpression increased both the percentages and numbers of GC B cells (Figures 2C–2E) with little effect on B cell proliferation (Figure S2A) but did not affect those of $CXCR5^{hi}Bcl6^{hi}$ Tfh cells (Figures S2B–S2D). Because MD4 Ig transgene could not undergo class switching in B cells, we next transduced Ascl2 retrovirus in LPS-activated B cells isolated from C57BL/6 mice before transferring into μMT mice. Seven days after 4-hydroxy-3-nitrophenyl (NP)-KLH immunization, the total levels of NP-KLH-specific IgG, IgG1, and IgG2a, but not IgM, significantly increased in the sera of mice receiving Ascl2-transduced B cells compared with control virus-infected B cells (Figure 2F). The ratios of high-affinity anti-NP (NP_4) antibodies to total anti-NP (NP_{29}) antibodies, a measurement for affinity maturation, markedly increased in mice receiving *Ascl2*-transduced B cells, including total IgG, IgG1, and IgG2a (Figure 2G), whereas Tfh cell development was not affected by Ascl2 overexpression (Figures S2E–S2G). Consistent with the upregulation of *Aicda* mRNA by Ascl2 overexpression *in vitro*, AID expression was clearly higher in mice transduced by Ascl2 than control virus *in vivo* (Figure 2H).

To determine whether Ascl2 regulated GC B cells through a cell-intrinsic manner, MD4 B cells carrying different congenic markers and separately transduced with *Ascl2* or control virus were mixed at 1:1 ratio and then co-transferred into mice together with OT-II T cells. The recipient mice were then immunized with OVA-HEL and analyzed 7 days later. GC B cells were significantly increased in Ascl2-overexpressing B cells (Figure 2I).

These data together strongly suggest an important role by Ascl2 in regulating the differentiation and function of GC B cells.

Ascl2 expression in B cells is critical for GC responses

To further examine the role of Ascl2 in GC reactions, we generated B cell-specific *Ascl2*-deficient mice by crossing the $Ascl2^{fl/fl}$ mice with $CD19^{Cre}$ (henceforth referred to as Ascl2 knockout [KO] mice). *Ascl2* deficiency did not affect normal B cell development under homeostatic condition (Figures S3A and S3B). Comparing GC responses after KLH immunization

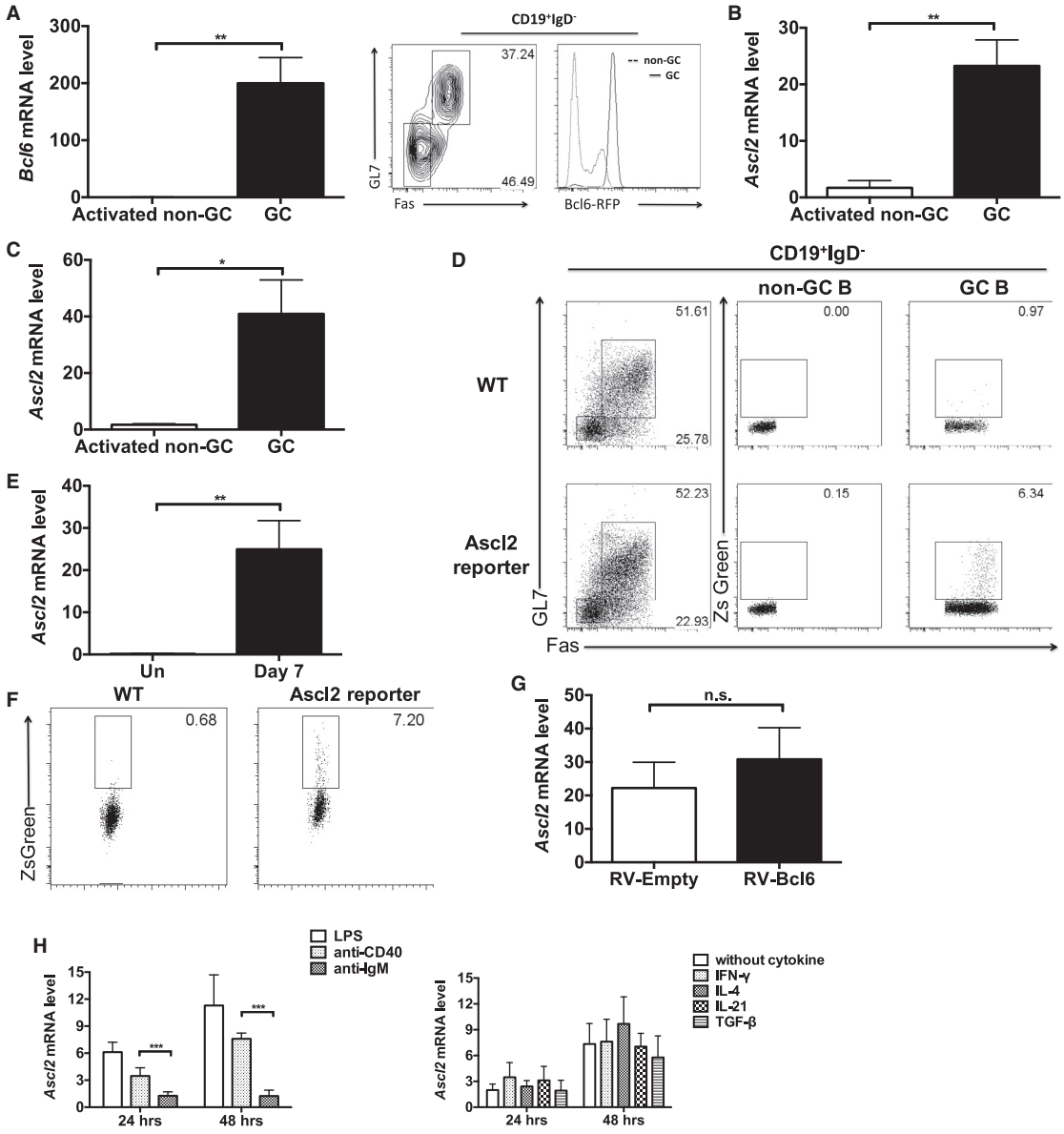

Figure 1. Expression of Ascl2 in germinal center (GC) B cells

(A) Both GC B (Fas^+GL7^+) and activated non-GC B (Fas^-GL7^-) cells were sorted from the draining lymph nodes of Bcl6-RFP mice immunized with KLH/CFA and then analyzed for mRNA expression of *Bcl6* by real-time RT-PCR or Bcl6-RFP reporter expression by flow cytometry among live lymphocytes.

(B) The mRNA expression of *Ascl2* in sorted GC B cells and activated non-GC B cells isolated in the KLH/CFA-immunized B6 mice.

(C) The mRNA expression of Ascl2 in sorted MD4 GC B and activated non-GC B cells isolated in the adoptive B cell transfer models.

(D) The Ascl2 ZsGreen reporter expression in GC B (Fas^+GL7^+) and activated non-GC B (Fas^-GL7^-) cells in draining lymph nodes of Ascl2 ZsGreen mice immunized with KLH/CFA. All the flow cytometry analysis was performed 7 days after immunization.

(E) The mRNA expression of Ascl2 or Ascl2-ZsGreen reporter expression in B cells activated and cultured *in vitro* with anti-IgM/anti-CD40 for 7 days.

(F) The Ascl2-Zs Green reporter expression in B cells activated and cultured *in vitro* with anti-IgM/anti-CD40 for 7 days by flow cytometry.

(G) The Ascl2 mRNA expression in B cells infected with RV-Empty or RV-Bcl6 retroviruses.

(H) The Ascl2 mRNA expression level in B cells cultured *in vitro* under various conditions as indicated. All the experiments were repeated at least three times with similar results.

between $Ascl2^{fl/fl}$ × $CD19^{WT}$ and $Ascl2^{WT/WT}$ × $CD19^{WT}$ mice, Ascl2 gene appeared to be fully functional in the absence of the Cre expression (Figure S3C). Upon immunization with NP-KLH, compared with the wild-type (WT) $CD19^{Cre}$ control mice, the frequencies and numbers of GC B cells were significantly reduced in *Ascl2* KO mice 7 days following immunization (Figures 3A–3C), whereas the numbers and frequencies of $CXCR5^{hi}Bcl6^{hi}$ Tfh cells were not affected (Figures S3D–S3F).

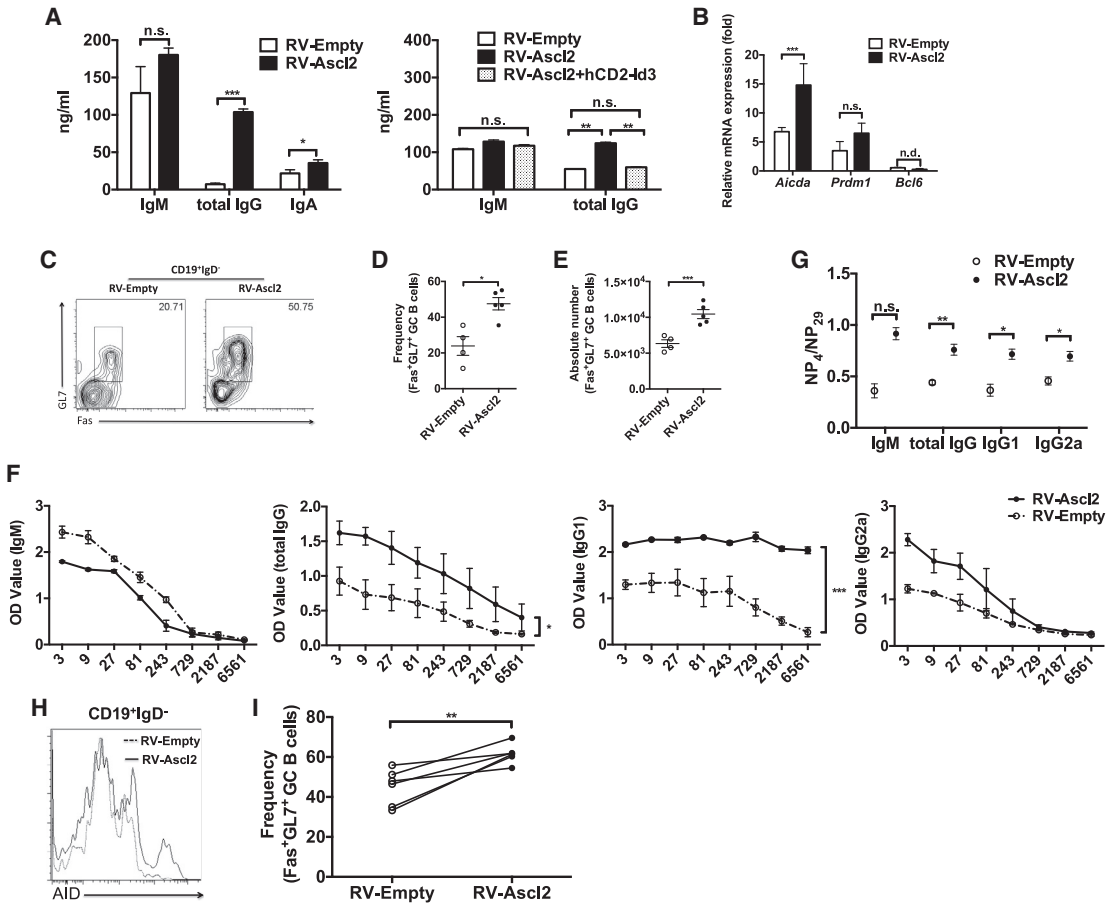

Figure 2. Ascl2 promotes GC B cell development

(A) The level of IgM, total IgGs, and IgA in the supernatants of *in vitro*-cultured B cells infected with the RV-Empty or RV-Ascl2 retroviruses, as examined by ELISA; when indicated, B cells were infected with both RV-Ascl2 and hCD2-Id3 retroviruses and analyzed for antibody production.

(B) Expression of *Aicda*, *Blimp1*, and *Bcl6* in RV-Ascl2 or RV-Empty virus-infected B cells in (A).

(C–E) Naive MD4 B cells were activated *in vitro*, infected with RV-Ascl2 or RV-Empty retroviruses, and then transferred into CD45.1 recipient mouse (n = 5) together with naive OT-II T cells, followed by immunization with OVA-HEL/CFA. The donor MD4 B cells were isolated from draining lymph nodes 7 days later and analyzed for GC B cell development: (C) flow cytometry data of donor GC B cells (live $CD19^+IgD^-GL7^+Fas^+$); (D) the frequencies of GC B cells in (C); and (E) the numbers of GC B cells in (C).

(F) KLH-specific antibodies in the sera of μMT mice receiving RV-Ascl2- or RV-Empty retrovirus-transduced B cells and immunized by NP-KLH/CFA immunization. x axis indicates the 3-fold serial dilutions of serum samples.

(G) Antibody affinity maturation of IgM, total IgGs, IgG1, and IgG2a antibody in (F). The Ig affinity maturation index was defined by the ratios of anti-NP_4 versus anti-NP_{29} antibody titers.

(H) Flow cytometry data of AID expression in (F).

(I) The frequencies of RV-Ascl2-transduced CD45.1 B cells and RV-Empty retrovirus-infected CD45.2 B cells in the μMT mice immunized with KLH/CFA. All the experiments were repeated at least two to three times with consistent results.

Of note, the ratio of $CXCR4^{hi}CD86^{lo}$ centroblasts to $CXCR4^{lo}CD86^{hi}$ centrocytes was altered in the absence of *Ascl2* (Figures 3D and 3E). In addition, histological analysis showed relatively smaller GC sizes in *Ascl2* KO mice (Figures 3F and 3G). Consistent with the GC defects, serum levels of antigen-specific Igs, including total IgG, IgG1, and IgG2a, significantly reduced in *Ascl2* KO mice (Figure 3H), as well as the ratios of high-affinity anti-NP_4 versus anti-NP_{29} antibodies (Figure 3I).

We further examined the intrinsic function of Ascl2 in B cells via adoptive B cell transfer experiments, when $CD19^{Cre}$ and *Ascl2* KO B cells were co-transferred into μMT recipients. *Ascl2* deficiency led to ~40%–50% reduction in the frequencies or numbers of GC B cells compared with the co-transferred control $CD19^{Cre}$ B cells in the draining lymph nodes (LNs) followed by NP-KLH immunization (Figure 3J). Simiar results were found in Peyer's patches under homeostatic condition (Figures S4A–S4C). This result was also confirmed by inducible deletion of *Ascl2* in activated B cells using the $Ert2^{Cre}$ system in the adoptive transfer experiment (Figures S5A–S5E). All the defects in GC B cells were independent of the Tfh cell population (Figures S4D–S4F, S5F–S5H). In contrast, *Ascl2* deficiency in B cells did not

CellPress
OPEN ACCESS

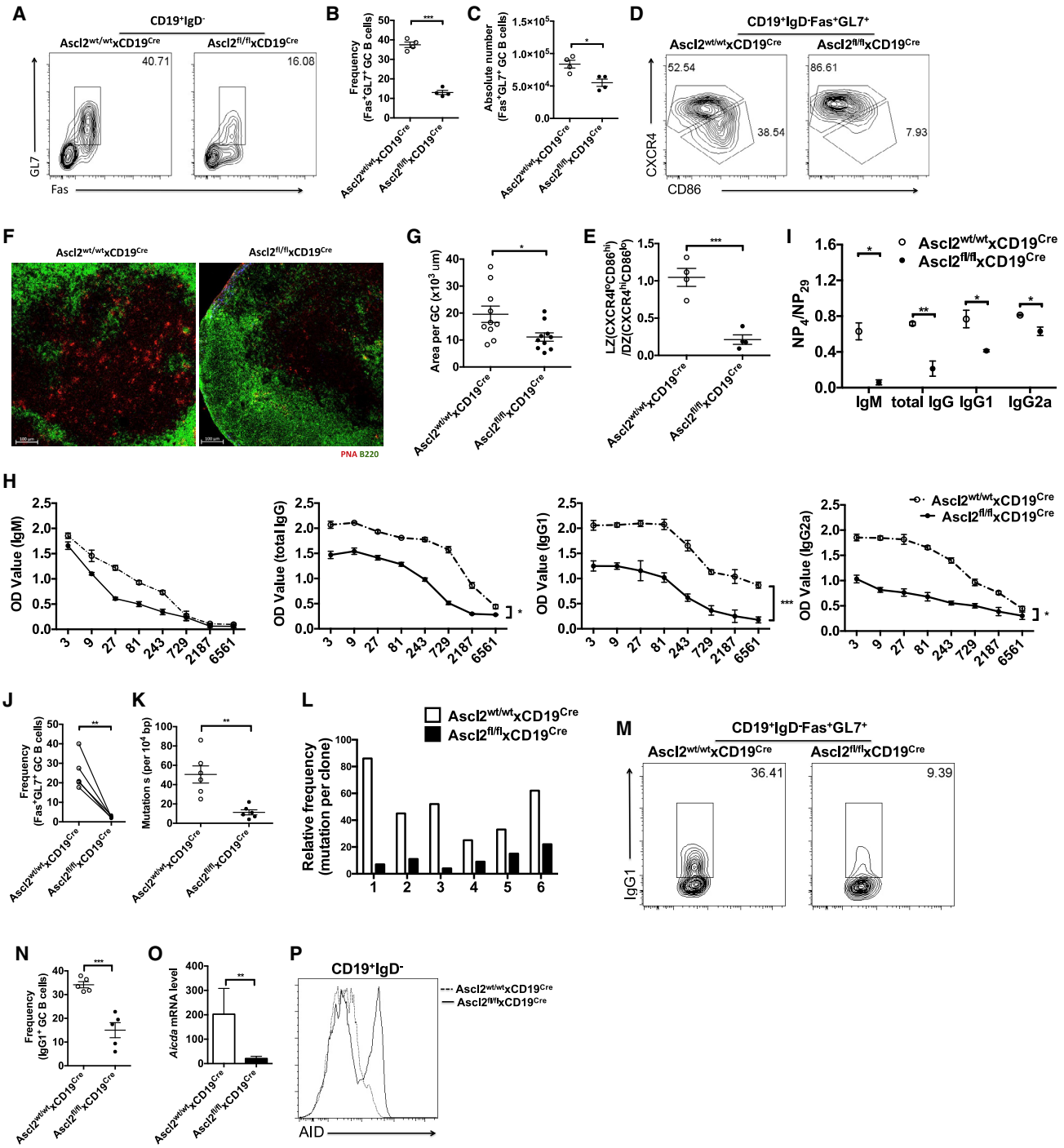

Figure 3. Ascl2 deficiency in B cells inhibits GC B cell development

$CD19^{Cre}$ and $Ascl2^{fl/fl}$ × $CD19^{Cre}$ mice were immunized with NP-KLH and analyzed 7 days later.

(A) GC B cells from draining lymph nodes as determined by live $CD19^{+}IgD^{-}Fas^{+}GL7^{+}$ staining.

(B and C) Frequencies and numbers of GC B cells.

(D) Flow cytometry data of $CXCR4^{hi}CD86^{lo}$ centroblasts versus $CXCR4^{lo}CD86^{hi}$ centrocytes (gated on $CD19^{+}IgD^{-}Fas^{+}GL7^{+}$ GC B cells).

(E) Statistical data on DZ (dark zone) ($CD86^{lo}CXCR4^{hi}$)/LZ (light zone) ($CD86^{hi}CXCR4^{lo}$) ratio.

(F) GC staining of peanut agglutinin (PNA) and B220 with draining lymph nodes section (scale bar, 100 μm).

(G) Statistical data on the size of each GC in (F) (pooled data from three independent experiments).

(H) Serum KLH-specific antibodies. x axis indicates the 3-fold serial dilutions of serum samples.

(legend continued on next page)

affect T cell-independent antibody response in the LPS/CFA-immunized model (Figures S3G–S3I). These data together highlight an important B cell-intrinsic role of Ascl2 in regulating GC B cell differentiation and function.

Because GC reaction is essential for somatic mutations and diversification of Ig repertoires, we next examined the frequencies of mutations in the J_H4-adjacent intronic region of IgH in WT (*CD19*^{Cre}) and *Ascl2* KO mice following NP-KLH immunization. The results showed that not only the overall mutation rates but also the frequencies of clones carrying multiple mutations were substantially decreased in Ascl2 KO mice (Figures 3K and 3L). Also, *Ascl2* deficiency in B cells lead to declined frequencies of IgG1$^+$ GC B cells, indicating deletion of Ascl2 lowered the CSR in GC B cells (Figures 3M and 3N). Consistent with the findings from Ascl2 overexpression assays, the *Aicda* mRNA level (Figure 3O) and AID (Figure 3P) were both significantly reduced in *Ascl2*-deficient GC B cells.

Loss of Ascl2 in B cells impairs host defense to influenza infection

To further address the function of Ascl2 in host defense, we infected *CD19*^{Cre} and *Ascl2* KO mice with influenza virus via intranasal administration. Compared with control mice, *Ascl2* KO mice showed significantly worsened weight loss and a delayed recovery, with ~3-fold more viral hemagglutinin (HA) mRNA expression in the lungs on day 9 following virus infection (Figure 4B). Further analysis showed Fas$^+$GL7$^+$ GC B cells were reduced by more than 90% in the lung draining LNs of *Ascl2* KO mice, in both frequencies and absolute numbers, along with significantly reduced serum levels of HA-specific IgG1 and total IgG, but not IgM or IgG2a (Figures 4C–4E). In contrast, B cell-specific *Ascl2* deficiency led to significantly increased CXCR5^{hi}Bcl6^{hi} Tfh cells in lung draining LNs (Figure S6A–S6C), likely because of compensatory mechanisms for defective GC B cell response. Also, GC B cells in the lung were reduced in *Ascl2*$^{fl/fl}$*CD19*^{Cre} mice (Figures S6D–S6F). Because *Ascl2* deficiency did not affect CD4$^+$ or CD8$^+$ T cell frequencies in the lung, draining LNs, and bronchoalveolar lavage fluid (BALF) (Figures S6G), our results together highlight an important protective role of Ascl2 in B cells and humoral immune response against viral infection.

Ascl2 regulates GC B cell gene expression

To understand the molecular mechanisms whereby Ascl2 regulates GC B cell development, we performed RNA sequencing (RNA-seq) assays with B cells transduced with Ascl2 overexpression or control vector. In total, Ascl2 overexpression altered the expression of 449 genes by ≥2-fold, with 293 upregulated and 156 downregulated (Figure 5A). Through comparison with previously published RNA-seq data of GC versus non-GC B cells (Cho et al., 2018), we found that 42 out of the 449 Ascl2-regulated genes were associated with GC B cell development, among which 34 were upregulated and 18 were downregulated by Ascl2 overexpression (Figures 5A–5C). Notably, a number of genes implicated in GC B cell development or GC response, including *Aicda*, *Ung*, *Dnmt1*, *Gna13*, and *Batf*, were among the top genes upregulated by Ascl2. However, the genes involved in plasma and memory B cell development and function, including *Klf2* and *Cd70*, were greatly suppressed by Ascl2.

Consistently, in the KLH immunization model, in sorted GC cells, B cell-specific deletion of *Ascl2* reduced the expression of *Aicda*, *Ung*, and *Gna13*, as well as several other genes involved in GC B cell formation and function, including *Bax*, *Adam17*, *Socs1*, *Batf*, *Irf4*, and *Foxp1* (Figure 5D). Notably, *Ascl2* deficiency also reduced the expression of *Lef1*, a transcription factor essential for Tfh cell differentiation (Choi et al., 2015), and *Rictor*, the core component of mTORC2. These data support an important role of Ascl2 in regulating the development and function of GC B cells.

AID serves as a critical functional target of Ascl2 in GC B cell response

To determine the genes directly regulated by Ascl2 in B cells, we performed genome-wide Ascl2 chromatin immunoprecipitation sequencing (ChIP-seq) with GC B cells isolated from draining LNs of NP-KLH-immunized B6 mice. In total, Ascl2 bound 996 genes, among which 41% and 36% fell into the intronic (blue) and intergenic (red) regions, respectively, with only 14% of Ascl2 binding sites located in the promoter regions (green) (Figure 6A). Interestingly, 56 of 996 Ascl2-bound genes were also regulated by Ascl2 based on our RNA-seq data (Figure 6B), including chemokine receptors *Cxcr4* and *Cxcr5*, transcription factor *Batf* and *Irf4*, and receptor signaling regulators *Gna13*, *Tab2*, and *Rgs13* (Figure 6C), suggesting a direct regulation, whereas *Bcl6* and *Prdm1* were not bound or regulated by *Ascl2*. In line with the nature of Ascl2 as an E-box protein, the ASCL2-binding peaks were enriched with the E-box protein-binding motif (5′-CANNTG-3′) (Figure 6D).

Considering the importance of Bcl6 in GC B cell differentiation, we also compared genome-wide occupancies of Ascl2 versus Bcl6 as reported in previous studies (Hatzi et al., 2013). Interestingly, ~30% of ASCL2-bound genes were correlated with BCL6 binding peaks (Figure 6E). Consistent with our earlier findings in T cells, Ascl2 and Bcl6 showed no reciprocal binding at their loci (Figures 6F and 6G), suggesting parallel or synergistic effects in regulating genes involved in GC B cell development. Ascl2 can form heterodimers with three other basic-helix-loop-helix (bHLH) family members, including E2-2 (also known as TCF4), E47 (also known as TCF3), and HEB (also known as TCF12) in human cells. Consistently, Ascl2 shared a large portion of commonly bound genes with E47 in B cells, including *Batf*,

(I) Antibody affinity maturation of IgM, total IgGs, IgG1, and IgG2a antibodies as determined by the ratios of anti-NP_4 versus anti-NP_{29} antibody titers.
(J–O) Naive B cells from CD45.1$^+$MD4xAscl2$^{wt/wt}$ × CD19^{Cre} and CD45.2$^+$MD4xAscl2$^{fl/fl}$ × CD19^{Cre} were co-transferred into μMT mice with naive T cells from OT-II mice, followed by immunization with OVA-HEL/CFA, and the recipient mice were then analyzed 7 days later. (J) Statistical data on Fas$^+$GL7$^+$ GC B cells in the μMT recipient mice. (K) The frequencies of mutations in the J_H4-adjacent intronic region. (L) The frequencies of clones carrying multiple mutations. (M and N) Flow cytometry and statistical data of IgG1$^+$ GC B cells. (O) *Aicda* mRNA expression in GC B cells.
(P) Flow cytometry data of AID expression in (A).
All data were representative of three independent experiments.

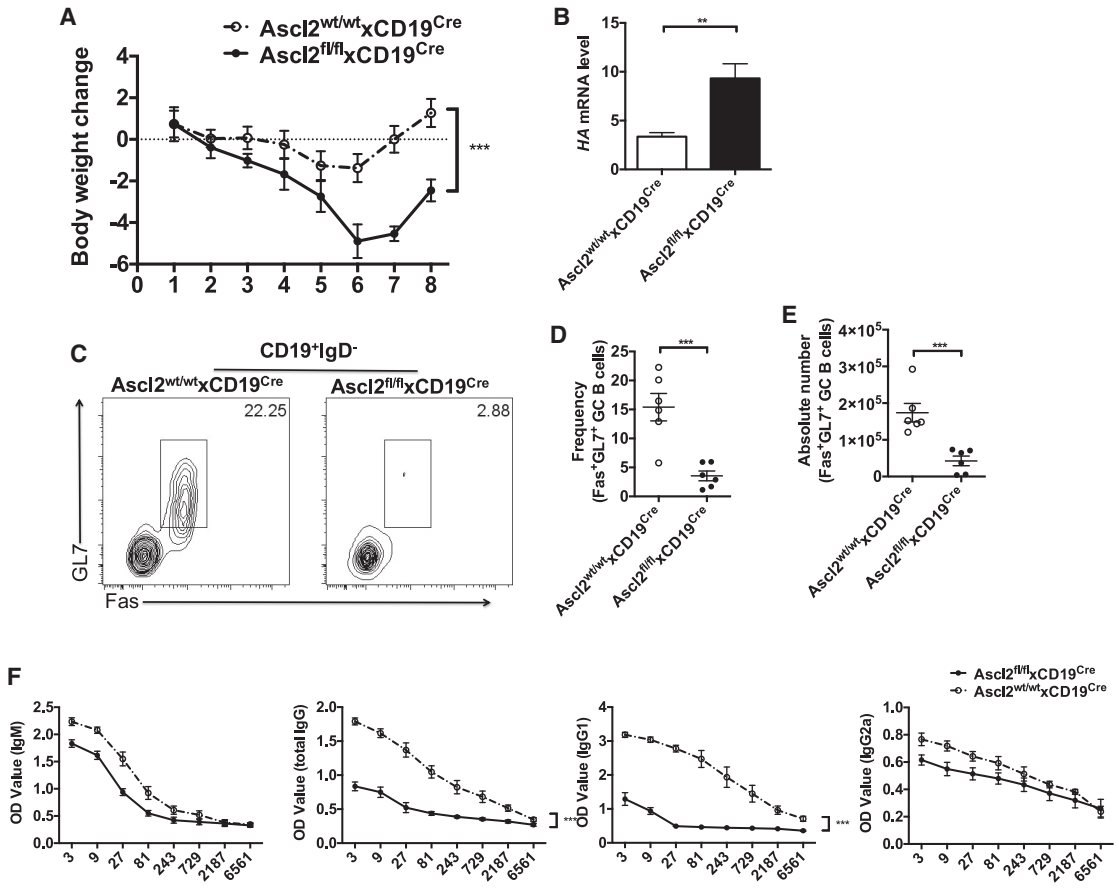

Figure 4. *Ascl2* deficiency in B cells impairs host defense against influenza infection

(A) Body weight loss of $CD19^{Cre}$ and $Ascl2^{fl/fl}$ × $CD19^{Cre}$ mice.

(B) The viral gene expression in the lung 8 days after virus infection as determined by the relative mRNA expression of viral HA gene.

(C) GC B cells (Fas^+GL7^+) in the lung draining lymph nodes from influenza-infected mice.

(D) The frequencies of GC B cells in (C).

(E) The absolute numbers of GC B cells in (C).

(F) Serum levels of virus-specific IgM, total IgGs, IgG1, and IgG2a measured by ELISA. x axis indicates the 3-fold serial dilutions of serum samples.

All data were representative of three independent experiments.

Cxcr5, and *Cxcr4* (Figures 6H and 6I). Interestingly, the *Aicda* locus was bound by both Ascl2 and E47, but their binding peaks were located at distinct regions, indicating an independent or synergistic role of Ascl2 and E47 in regulating Aicda expression (Figure 6J).

Finally, the binding of Ascl2 to the *Aicda* gene locus was confirmed by ChIP-qPCR assays, and Ascl2 selectively bound the conserved non-coding sequence 2 (CNS2) region of *Aicda* genes identified in previous studies (Gloury et al., 2016; Wöhner et al., 2016) (Figure 6K). To determine if the binding of Ascl2 is functional, the CNS1-CNS4 sequences at the *Aicda* loci were individually fused to the *Aicda* promoter sequence in the PGL3-reporter plasmid. In the dual-luciferase reporter assays, only CNS2 could induce robust *Aicda* reporter activity, further enhanced by Ascl2 (Figure 6L), consistent with the ChIP-seq findings.

To assess whether AID is a functional target of Ascl2, we conducted retroviral expression of *Aicda* in *Ascl2*-deficient B cells, which was sufficient in rescuing B cell defect caused by *Ascl2* deficiency, as determined by the generation of $IgG1^+$ activated B cells *in vitro* for 3 days (Figures 6M and 6N). This result thus highlights an important role of AID in Ascl2-dependent GC B cell response.

DISCUSSION

We have previously shown that Ascl2 plays an important role in regulating Tfh cell differentiation through regulating CXCR5 expression and early Tfh cell migration (Liu et al., 2014). In this study, we examined the role of Ascl2 in GC B cells. Ascl2 was found to be significantly and selectively increased in GC, but not non-GC B cells. In addition, Ascl2 overexpression significantly enhanced the function of B cells *in vitro* or *in vivo*, whereas B cell-specific Ascl2 deficiency dampened GC B cell formation and humoral response. Our study thus revealed a critical role of Ascl2 in regulating GC reactions, in a B cell-intrinsic manner.

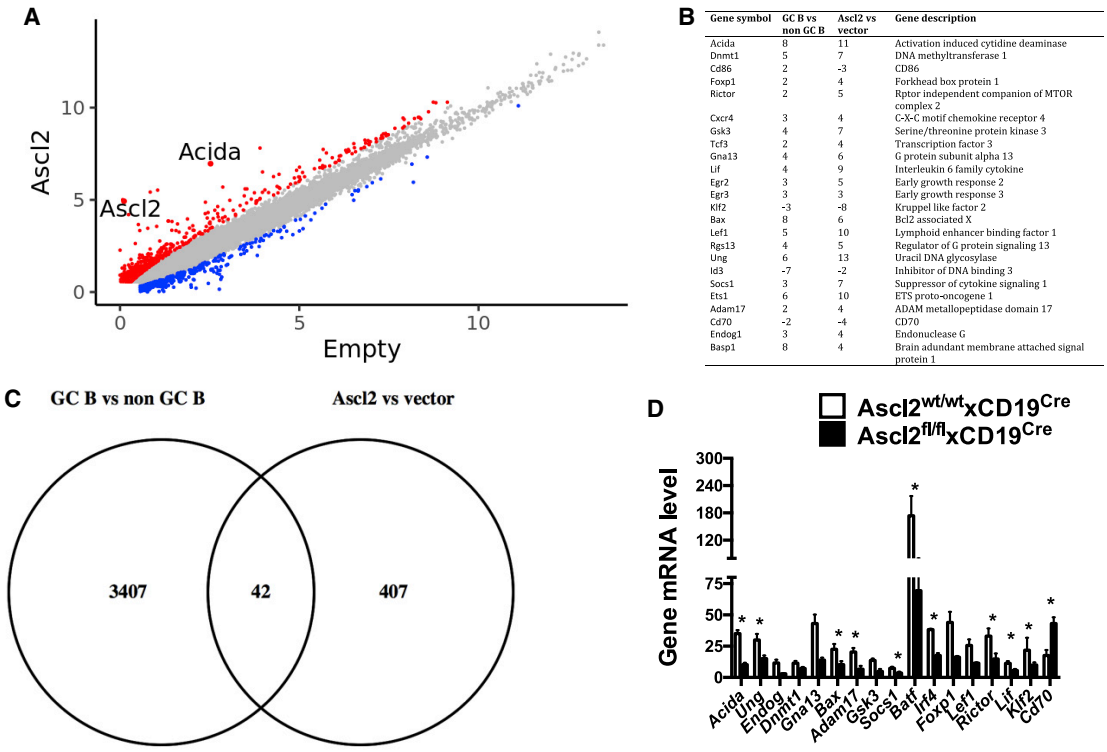

Figure 5. Ascl2 regulates GC B cell-related genes

Total mRNA was extracted from *in vitro*-cultured B cells infected with the RV-Empty or RV-Ascl2 retroviruses sorted with GFP marker.

(A) The scatterplot of RNA-seq data obtained with B cells transduced with RV-Ascl2 or RV-Empty retroviruses with FPKM as x-y axis. The green line indicated gene expression change ≥2-fold.

(B) Top list of genes altered by Ascl2 overexpression.

(C) Venn diagram of genes regulated by Ascl2 versus GC B cell-related genes.

(D) Transcriptional expression of *Aicda*, *Ung*, *Endog*, *Dnmt1*, *Gna13*, *Bax*, *Adam17*, *Gsk3*, *Socs1*, *Batf*, *Irf4*, *Foxp1*, *Lef1*, *Rcitor*, *Lif*, *Klf2*, and *Cd70* in GC B cells isolated from the draining lymph nodes of KLH-immunized Ascl2$^{fl/fl}$ × CD19^{Cre} or CD19^{Cre} control mice as measured by RT-PCR. Data are representative of three independent experiments.

In this work, the immune defense against influenza virus in B cell-specific Ascl2-deleted mice may also reflect more beyond compromised GC antibody responses. The body weight loss data suggested that virus replication is probably less well attenuated prior to the time when GC antibodies would be present (prior to day 7). In addition, Ascl2 expression can be induced *in vitro* in activated B cells stimulated with anti-IgM and anti-CD40; thus, there may be some function of Ascl2 on the extrafollicular antibody response.

A recent study showed class switch largely happened prior to the formation of a GC (Roco et al., 2019). Consistent with this report, we detected peak of Ascl2 expression (96 h after immunization) preceded the formation of GCs (data not shown). These results indicated Ascl2 could function in CSR even before GC formation.

The AID, encoded by the *Aicda* gene, is known as the master regulator for secondary antibody diversification through driving SHM and CSR. The expression of *Aicda* in B cells is regulated by E-box proteins through their binding to multiple regulatory regions within the *Aicda* gene locus: E2a-encoding transcription factors E12 and E47 bind enhancer regions 4 and 5 (E4 and E5), respectively, and E2-2 that binds E2, respectively. The *E2a* gene deletion disrupts rearrangement of immunoglobin genes and causes a severe blockade of B cell development between the pre-B and pro-B cell stages (Bain et al., 1994; Zhuang et al., 1994). Additional studies show that E47 and E12 are also expressed in mature B cells, particularly in the centroblasts of GC B cells (Goldfarb et al., 1996), suggesting a role in regulating GC response. Indeed, the combined deletion of E2A and E2-2 results in a complete deficit in antigen-induced B cell differentiation (Gloury et al., 2016; Wöhner et al., 2016). ASLC2 is also an E-box-containing protein, and our studies showed that its overexpression could increase *Aicda* transcription in B cells, whereas its deficiency in B cells significantly reduced *Aicda* expression and led to a severe defect in CSR and SHM during humoral response. Mechanistically, ASCL2 was found to directly bind to the CNS2 region at the *Aicda* locus, a regulatory region not occupied by E47. Although it was previously reported that Asc proteins bind to DNA as heterodimers in fly, our overexpression experiment suggested that it could function as homodimers in mice. Also, ChIP-seq data revealed that the binding sites for Ascl2 in *Aicda* were different from those for other E-box protein family members, including E47 and E2-2. Besides, studies on E47

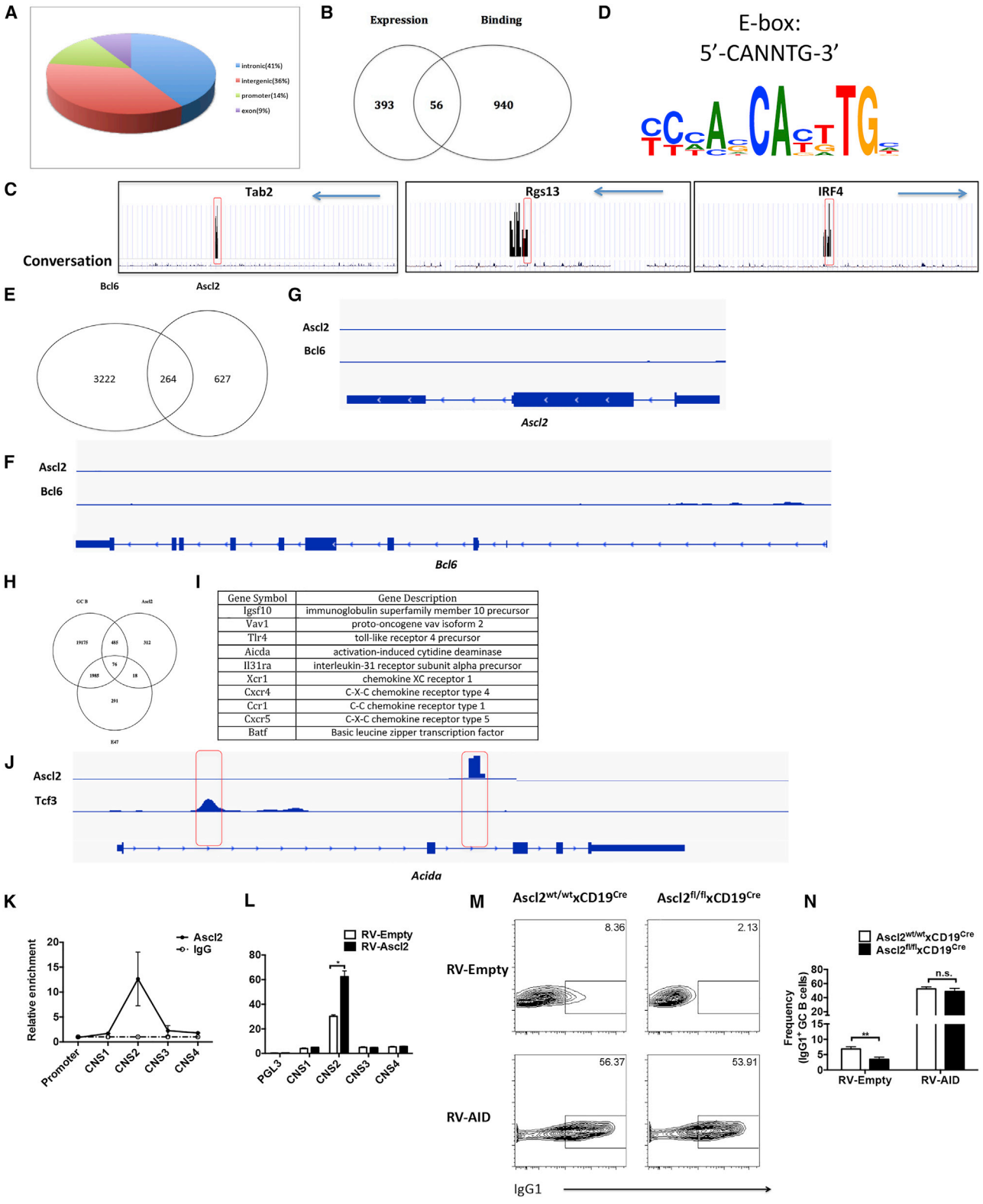

(legend on next page)

and E2-2 (Gloury et al., 2016; Wöhner et al., 2016) did not show co-occupancy. Interestingly, the defective humoral response caused by *Ascl2* deficiency, including decrease in antibody-producing cells, could be completely rescued by *Aicda* overexpression in B cells, even when we analyzed the cell population with intermediate expression levels. Our study thus identified Ascl2 as an essential AID regulator in controlling GC reactions.

It is noted that AID mutant patients often develop various autoimmune syndromes, including arthritis, autoimmune hepatitis, and Crohn's disease (Quartier et al., 2004), whereas AID deficiency also exacerbates autoimmune syndromes in Lpr mice, as evidenced by elevated production of autoantibodies and enhanced glomerulonephritis (Chen et al., 2010). In contrast, B cell-specific Ascl2 deficiency did not affect normal B cell development under homeostasis status and even declined GC B cell responses under immune challenge conditions. The mechanisms underlying the phenotypic differences between *Aicda* and *Ascl2* deficiency are not clear yet, which warrants further investigation in the future.

Bcl6 serves as a master transcriptional factor controlling the development of both GC T and GC B cells. In B cells, Bcl6 plays an important role in promoting the rapid proliferation of GC B cells and facilitating their tolerance to high rates of SHM. Based on our previous study (Liu et al., 2014) and the results in this study, Ascl2 could also regulate both GC T and GC B cell development, but via distinct mechanisms. Although in this study, Ascl2 and Bcl6 showed no reciprocal binding at the other loci, which could exclude the possibility that Ascl2 may regulate these genes through enhancers that may interact with the gene promoter to form a local promoter-enhancer interactome and function as one cooperative regulatory unit to induced Bcl6 expression. Through comparing the ChIP-list of ASCL2 and BCL6 targeted genes in B cells, we found that Bcl6 bound ~3.5-fold more genes than Ascl2 (3,796 versus 996 genes), indicating a broader role of Bcl6 than Ascl2 in B cells. It is also noted that ~30% of genes bound by Ascl2 are also targeted by Bcl6, suggesting the two transcription factors may have synergistic or redundant functions in regulating the development or function of GC B cells, which may need to be further investigated.

In summary, our studies identified Ascl2 as a transcription factor that is induced in GC B cells and critically controls GC B cell differentiation via direct regulation of AID expression. The findings in this study extend the role of Ascl2 and are useful for understanding the molecular mechanisms controlling GC reactions and humoral responses.

STAR★METHODS

Detailed methods are provided in the online version of this paper and include the following:

- KEY RESOURCES TABLE
- RESOURCE AVAILABILITY
  - Lead contact
  - Materials availability
  - Data and code availability
- EXPERIMENTAL MODEL AND SUBJECT DETAILS
  - Mice
- METHOD DETAILS
  - B cell isolation, transfer, and culture assays
  - ELISA assay
  - Real-time RT–PCR analysis
  - Retroviral transduction
  - KLH, NP-KLH and OVA-HEL immunization
  - Flow Cytometry
  - Immunofluorescence staining
  - Immunoglobulin sequence analysis
  - Influenza virus infection
  - High-throughput sequencing and ChIP-seq
- QUANTIFICATION AND STATISTICAL ANALYSIS
  - Statistics

SUPPLEMENTAL INFORMATION

Supplemental information can be found online at https://doi.org/10.1016/j.celrep.2021.109188.

ACKNOWLEDGMENTS

This work was supported by grants from National Key Research and Development Program of China (2016YFC0906200 to C.D.), National Natural Science

Figure 6. ASCL2 directly regulates Aicda expression

$CD19^+IgD^-Fas^+GL7^+$ GC B cells were isolated from draining lymph nodes of KLH/CFA-immunized B6 mice for 7 days and used for ChIP-seq library construction.
(A) Distribution of ASCL2 ChIP-seq peaks in B cells.
(B) Venn diagram of genes regulated by Ascl2 versus ASCL2-binding genes obtained from RNA-seq and ASCL2-ChIP-seq data, respectively.
(C) ASCL2-ChIP peaks at the *Tab2*, *Rgs13*, and *Irf4* gene loci.
(D) E-box motif enriched in ASCL2 binding peaks.
(E) Venn diagram of ASCL2 versus BCL6 ChIP-seq peaks.
(F and G) Distribution of ASCL2 versus BCL6 ChIP-seq peaks by Ascl2 and Bcl6 at the *Bcl6* and *Ascl2* gene loci.
(H) Venn diagram of ASCL2 and E47 ChIP-seq peaks (reanalyzed based on E47 ChIP-seq data from Dominguez-Sola et al., (2015) report; GEO: GSM1668937) versus the RNA-seq obtained from GC B cells versus non-GC B cells in the previous report.
(I) GC B cell-related genes commonly regulated by both Ascl2 and E47.
(J) Distribution of ASCL2 and E47 ChIP-seq peaks at the *Aicda* locus.
(K) Binding of ASCL2 to the *Aicda* locus in GC B cells as determined by ChIP-qPCR.
(L) The CNS2-Aicda luciferase reporter activity in A20 B cells transfected with RV-Ascl2 or RV-Empty plasmids.
(M) Naive B cells isolated from $Ascl2^{fl/fl}CD19^{Cre}$ or $CD19^{Cre}$ mice were pre-activated with anti-IgM/anti-CD40, transduced with RV-Empty or RV-AID, and then examined for IgG1 expression 7 days later in *in vitro* cultures by flow cytometry.
(N) The frequencies of $IgG1^+$ B cells in (M). Data are representative of three independent experiments.

Foundation of China (31630022, 31821003, and 31991170 to C.D.), and Beijing Municipal Science and Technology (Z181100001318007 to C.D.). We also thank the flow cytometry core facility (Institute for Immunology), the animal platform at Tsinghua University, and members of the Dong laboratory for technical support and assistance.

AUTHOR CONTRIBUTIONS

L.S. designed and performed the experiments and wrote the manuscript. B.Z., X.L., and H.W. generated the Ascl2 ZsGreen mice. X.Z. contributed to the data analysis of RNA-seq and ChIP-seq. W.J. contributed to design and performed the experiments. X.W. reviewed and edited the manuscript. C.D. designed the research and edited the manuscript.

DECLARATION OF INTERESTS

The authors declare no competing interests.

Received: January 9, 2020
Revised: August 14, 2020
Accepted: May 7, 2021
Published: June 1, 2021

REFERENCES

Bain, G., Maandag, E.C.R., Izon, D.J., Amsen, D., Kruisbeek, A.M., Weintraub, B.C., Krop, I., Schlissel, M.S., Feeney, A.J., van Roon, M., et al. (1994). E2A proteins are required for proper B cell development and initiation of immunoglobulin gene rearrangements. Cell *79*, 885–892.

Basso, K., and Dalla-Favera, R. (2012). Roles of BCL6 in normal and transformed germinal center B cells. Immunol. Rev. *247*, 172–183.

Chen, L., Guo, L., Tian, J., Zheng, B., and Han, S. (2010). Deficiency in activation-induced cytidine deaminase promotes systemic autoimmunity in lpr mice on a C57BL/6 background. Clin. Exp. Immunol. *159*, 169–175.

Cho, S., Lee, H.M., Yu, I.S., Choi, Y.S., Huang, H.Y., Hashemifar, S.S., Lin, L.L., Chen, M.C., Afanasiev, N.D., Khan, A.A., et al. (2018). Differential cell-intrinsic regulations of germinal center B and T cells by miR-146a and miR-146b. Nature communications *9*, 2757.

Choi, Y.S., Gullicksrud, J.A., Xing, S., Zeng, Z., Shan, Q., Li, F., Love, P.E., Peng, W., Xue, H.H., et al. (2015). LEF-1 and TCF-1 orchestrate T(FH) differentiation by regulating differentiation circuits upstream of the transcriptional repressor Bcl6. Nature Immunology *16*, 980–990.

Cogné, M. (2013). Activation-induced deaminase in B lymphocyte maturation and beyond. Biomed. J. *36*, 259–268.

Cogné, M., Lansford, R., Bottaro, A., Zhang, J., Gorman, J., Young, F., Cheng, H.L., and Alt, F.W. (1994). A class switch control region at the 3′ end of the immunoglobulin heavy chain locus. Cell *77*, 737–747.

Deng, L.H., Zeng, Y.L., Feng, P., Liu, Y.L., Wang, L.C., Bai, Y., Tang, H., et al. (2012). Clinical characteristics of critical patients with pandemic influenza A (H1N1) virus infection in Chengdu, China. J Zhejiang Univ Sci B *13*, 49–55.

Dent, A.L., Shaffer, A.L., Yu, X., Allman, D., and Staudt, L.M. (1997). Control of inflammation, cytokine expression, and germinal center formation by BCL-6. Science *276*, 589–592.

Dominguez-Sola, D., Kung, J., Holmes, A.B., Wells, V.A., Mo, T., Basso, K., and Dalla-Favera, R. (2015). The FOXO1 Transcription Factor Instructs the Germinal Center Dark Zone Program. Immunity *43*, 1064–1074.

Gitlin, A.D., Shulman, Z., and Nussenzweig, M.C. (2014). Clonal selection in the germinal centre by regulated proliferation and hypermutation. Nature *509*, 637–640.

Gloury, R., Zotos, D., Zuidscherwoude, M., Masson, F., Liao, Y., Hasbold, J., Corcoran, L.M., Hodgkin, P.D., Belz, G.T., Shi, W., et al. (2016). Dynamic changes in Id3 and E-protein activity orchestrate germinal center and plasma cell development. J. Exp. Med. *213*, 1095–1111.

Goldfarb, A.N., Flores, J.P., and Lewandowska, K. (1996). Involvement of the E2A basic helix-loop-helix protein in immunoglobulin heavy chain class switching. Mol. Immunol. *33*, 947–956.

Hatzi, K., Jiang, Y., Huang, C., Garrett-Bakelman, F., Gearhart, M.D., Giannopoulou, E.G., Zumbo, P., Kirouac, K., Bhaskara, S., Polo, J.M., et al. (2013). A hybrid mechanism of action for BCL6 in B cells defined by formation of functionally distinct complexes at enhancers and promoters. Cell Rep. *4*, 578–588.

Liu, X., Yan, X., Zhong, B., Nurieva, R.I., Wang, A., Wang, X., Martin-Orozco, N., Wang, Y., Chang, S.H., Esplugues, E., et al. (2012). Bcl6 expression specifies the T follicular helper cell program in vivo. J. Exp. Med. *209*, 1841–1852, S1–S24.

Kwon, K., Hutter, C., Sun, Q., Bilic, I., Cobaleda, C., Malin, S., and Busslinger, M. (2008). Instructive role of the transcription factor E2A in early B lymphopoiesis and germinal center B cell development. Immunity *28*, 751–762.

Liu, X., Chen, X., Zhong, B., Wang, A., Wang, X., Chu, F., Nurieva, R.I., Yan, X., Chen, P., van der Flier, L.G., et al. (2014). Transcription factor achaete-scute homologue 2 initiates follicular T-helper-cell development. Nature *507*, 513–518.

Muramatsu, M., Kinoshita, K., Fagarasan, S., Yamada, S., Shinkai, Y., and Honjo, T. (2000). Class switch recombination and hypermutation require activation-induced cytidine deaminase (AID), a potential RNA editing enzyme. Cell *102*, 553–563.

Murre, C. (2005). Helix-loop-helix proteins and lymphocyte development. Nature Immunology *6*, 1079–1086.

Pinaud, E., Khamlichi, A.A., Le Morvan, C., Drouet, M., Nalesso, V., Le Bert, M., and Cogné, M. (2001). Localization of the 3′ IgH locus elements that effect long-distance regulation of class switch recombination. Immunity *15*, 187–199.

Pinaud, E., Marquet, M., Fiancette, R., Péron, S., Vincent-Fabert, C., Denizot, Y., and Cogné, M. (2011). The IgH locus 3′ regulatory region: Pulling the strings from behind. Adv. Immunol. *110*, 27–70.

Quartier, P., Bustamante, J., Sanal, O., Plebani, A., Debré, M., Deville, A., Litzman, J., Levy, J., Fermand, J.P., Lane, P., et al. (2004). Clinical, immunologic and genetic analysis of 29 patients with autosomal recessive hyper-IgM syndrome due to Activation-Induced Cytidine Deaminase deficiency. Clin. Immunol. *110*, 22–29.

Revy, P., Muto, T., Levy, Y., Geissmann, F., Plebani, A., Sanal, O., Catalan, N., Forveille, M., Dufourcq-Labelouse, R., Gennery, A., et al. (2000). Activation-induced cytidine deaminase (AID) deficiency causes the autosomal recessive form of the Hyper-IgM syndrome (HIGM2). Cell *102*, 565–575.

Roco, J.A., Mesin, L., Binder, S.C., Nefzger, C., Gonzalez-Figueroa, P., Canete, P.F., Ellyard, J., Shen, Q., Robert, P.A., Cappello, J., et al. (2019). Class-Switch Recombination Occurs Infrequently in Germinal Centers. Immunity *51*, 337–350.e7.

Sayegh, C.E., Quong, M.W., Agata, Y., and Murre, C. (2003). E-proteins directly regulate expression of activation-induced deaminase in mature B cells. Nature Immunology *4*, 586–593.

van der Flier, L.G., van Gijn, M.E., Hatzis, P., Kujala, P., Haegebarth, A., Stange, D.E., Begthel, H., van den Born, M., Guryev, V., Oving, I., et al. (2009). Transcription factor achaete scute-like 2 controls intestinal stem cell fate. Cell *136*, 903–912.

Vincent-Fabert, C., Fiancette, R., Pinaud, E., Truffinet, V., Cogné, N., Cogné, M., and Denizot, Y. (2010). Genomic deletion of the whole IgH 3′ regulatory region (hs3a, hs1,2, hs3b, and hs4) dramatically affects class switch recombination and Ig secretion to all isotypes. Blood *116*, 1895–1898.

Wikström, I., Forssell, J., Goncalves, M., Colucci, F., and Holmberg, D. (2006). E2-2 regulates the expansion of pro-B cells and follicular versus marginal zone decisions. J Immunol. *177*, 6723–6729.

Wöhner, M., Tagoh, H., Bilic, I., Jaritz, M., Poliakova, D.K., Fischer, M., and Busslinger, M. (2016). Molecular functions of the transcription factors E2A and E2-2 in controlling germinal center B cell and plasma cell development. J. Exp. Med. *213*, 1201–1221.

Yabuki, M., Ordinario, E.C., Cummings, W.J., Fujii, M.M., and Maizels, N. (2009). E2A acts in cis in G1 phase of cell cycle to promote Ig gene diversification. J. Immunol. *182*, 408–415.

Ye, B.H., Cattoretti, G., Shen, Q., Zhang, J., Hawe, N., de Waard, R., Leung, C., Nouri-Shirazi, M., Orazi, A., Chaganti, R.S., et al. (1997). The BCL-6 proto-oncogene controls germinal-centre formation and Th2-type inflammation. Nat. Genet. *16*, 161–170.

Zhuang, Y., Soriano, P., and Weintraub, H. (1994). The helix-loop-helix gene E2A is required for B cell formation. Cell *79*, 875–884.

STAR★METHODS

KEY RESOURCES TABLE

REAGENT or RESOURCE	SOURCE	IDENTIFIER
Antibodies		
Anti-IgM (clone RMM-1)	Biolegend	Cat# 406502; RRID:AB_315052
Anti-CD40 (clone FGK4.5)	Bioxcell	Cat# BP0016-2; RRID:AB_1107647
Anti-CD19 (clone 1D3)	eBioscience	Cat# 47-0193; RRID:AB_10853189
Anti-IgD (clone 11-26c.2a)	BD Biosciences	Cat# 563003; RRID:AB_2648353
anti-mouse IgM[a] (clone DS-1)	BD Biosciences	Cat# 553517; RRID:AB_394898
Anti-Fas(clone 15A7)	eBioscience	Cat# 53-0951; RRID:AB_10671269
Anti-GL7(clone GL-7)	eBioscience	Cat# 50-5902; RRID:AB_2574251
Anti-CD86 (clone GL1)	BD Biosciences	Cat# 560582; RRID:AB_1727518
Anti-CXCR4 (clone 2B11)	BD Biosciences	Cat# 562738; RRID:AB_2737757
Anti-CD4 (clone GK1.5)	eBioscience	Cat# 47-0041; RRID:AB_11218896
Anti-CD44 (clone IM7)	Biolegend	Cat# 103030; RRID:AB_830787
biotinylated Anti-CXCR5	BD Biosciences	Cat# 551960; RRID:AB_394301
Anti-PD-1(clone J43)	BD Biosciences	Cat# 551892; RRID:AB_394284
Anti-Bcl6(clone K112-91)	BD Biosciences	Cat# 562401; RRID:AB_11152084
Anti-B220(clone RA3-6B2)	BD Biosciences	Cat# 552772; RRID:AB_394458
Anti-CD45.1(clone A20)	eBioscience	Cat# 48-4053-82; RRID:AB_313504
Anti-CD45.2(clone 104)	eBioscience	Cat# 56-0454; RRID:AB_657752
Streptavidin	BD Biosciences	Cat# 554067; RRID:AB_10050396
Biotinylated Peanut Agglutinin (PNA)	Vector Labs	Cat#B-1075; RRID:AB_2313597
Anti-Achaete Scute homolog 2 Antibody (clone 7E2)	Millipore	Cat# MAB4418; RRID:AB_10561764
Goat anti-mouse IgM-HRP	SouthernBiotech	Cat# 1020-05; RRID:AB_2794201
Goat Anti-Mouse IgA-HRP	SouthernBiotech	Cat# 1040-05; RRID:AB_2714213
Goat Anti-Mouse IgG(H+L)-HRP	SouthernBiotech	Cat# 1036-05; RRID:AB_2794348
Goat Anti-Mouse IgG1-HRP	SouthernBiotech	Cat# 1071-05; RRID:AB_2794426
Goat Anti-Mouse IgG2a-HRP	SouthernBiotech	Cat# 0103-05; RRID:AB_2793886
Bacterial and virus strains		
Influenza virus (PR8, H1N1)	Deng et al., 2012	N/A
Chemicals, peptides, and recombinant proteins		
Fixable viability dye eFluor506	eBioscience	Cat# 65-0866
1X TMB Solution	eBioscience	Cat# 00-4201
Hen Egg Lysozyme (HEL)	Sigma	Cat# L6876
Albumin from chicken egg white (OVA)	Sigma	Cat# A5503
NP-KLH	Biosearch Technologies	Cat# N-5060
Keyhole Limpet Hemocyanin (KLH)	Sigma	Cat# H7017
Freund's Adjuvant Incomplete	Sigma	Cat# F5506
M. Tuberculosis Des. H37 Ra	BD	Cat# 231141
Recombinant Murine IFN-gamma	Peprotech	Cat# 315-05
Recombinant Murine IL-4	Peprotech	Cat# 214-14
Recombinant Murine IL-21	Peprotech	Cat# 210-21
Recombinant Human TGF-beta	R&D Systems	Cat# 240-B-010
Critical commercial assays		
Foxp3 / Transcription Factor Staining Buffer Set	eBioscience	Cat# 00-5523
NEXTflex TM ChIP-Seq DNA Sequencing Kit	Bioo Scientific	Cat# 5143

(*Continued on next page*)

Continued

REAGENT or RESOURCE	SOURCE	IDENTIFIER
NEXTflex Rapid RNA-Seq DNA Sequencing Kit	Bioo Scientific	Cat# 5138
Deposited data		
RNA-seq	This study	GSE169416
ChIP-seq	This study	GSE169416
Experimental models: Organisms/strains		
Mouse: C57BL/6J	Jackson Laboratory	JAX:000664
Mouse: Bcl6-RFP	Liu et al., 2012	N/A
Mouse: Ascl2$^{fl/fl}$	van der Flier et al., 2009	N/A
Mouse: Ascl2-ZS Green	This study	N/A
Mouse: CD19Cre: B6.129P2(C)-Cd19$^{tm1(cre)Cgn}$/J	Jackson Laboratory	JAX: 006785
Mouse: MD4: C57BL/6-Tg(IghelMD4)4Ccg/J	Jackson Laboratory	JAX: 002595
Mouse: OT-II: B6.CgTg(TcraTcrb)425Cbn/J	Jackson Laboratory	JAX: 4194
Mouse: CD45.1: B6.SJL-PtprcaPepcb/BoyJ	Jackson Laboratory	Jax: 002014
Software and algorithms		
FlowJo software v9.3.2	FlowJo LLC	https://www.flowjo.com/; RRID:SCR_008520
GraphPad Prism 6	GraphPad Software	https://www.graphpad.com/scientific-software/prism/

RESOURCE AVAILABILITY

Lead contact

Further information and requests for resources and reagents should be directed to and will be fulfilled by the Lead Contact, Chen Dong (chendong@tsinghua.edu.cn).

Materials availability

Reagents are commercially available and/or contacts for all materials are listed in Key resources table.

Data and code availability

Original RNA-seq and ChIP-seq data have been deposited to NCBI GSE169416.

EXPERIMENTAL MODEL AND SUBJECT DETAILS

Mice

All the mice were housed in specific pathogen-free animal facilities at Tsinghua University, and were used according to protocols approved by the Institutional Animal Care and Use Committee. The C57BL/6 mice were purchased from the animal platform at Tsinghua University. The CD19^{Cre}, MD4, OT-II mice were obtained from Jackson Laboratories. The Bcl6-RFP mice were previously described (Liu et al., 2012). The Ascl2fl/fl mice were generated previously (van der Flier et al., 2009) and bred with CD19-Cre to generate Ascl2$^{fl/fl}$xCD19^{Cre} and Ascl2$^{wt/wt}$xCD19^{Cre} control mice, or crossed with ETR2^{Cre} mice to generate Ascl2$^{fl/fl}$xETR2^{Cre} and Ascl2$^{wt/wt}$xETR2^{Cre} control mice. All the mice were female, and 6-8 wks old.

METHOD DETAILS

B cell isolation, transfer, and culture assays

B cells from mouse spleen or peripheral lymph nodes were prepared and isolated with a B cell Isolation Kit from Life Technologies by using the BD FACSAria III according to cell surface markers IgD and CD38. For adoptive B cell transfer experiment, 5x10^6 MD4 B cells of specific group were co-transferred into recipient mice together with 3x10^6 OT-II T cells. The immunization was performed 24 h later and the mice were analyzed 7 days post immunization. For *in vitro* cultures, naive B cells were cultured in RPMI-1640 medium supplemented with 10% FBS, 50 μM β-mercaptoethanol (Sigma-Aldrich), penicillin/streptomycin antibiotics (Invitrogen) and Non-Essential Amino Acids (Invitrogen), and activated and polarized using plate-bound coated 10 μg/mL anti-IgM and soluble anti-CD40 alone or plus IFN-γ, IL-4, IL-21 or TGF-β in order to drive class-switch.

ELISA assay

Various antibodies in the immunized mice or in B cell culture supernatants were detected by ELISA assays as reported(Liu et al., 2014). Briefly, themaxisorb plates (Nunc) were coated with 2 μg/mL Ig, 5 μg/mL KLH, 5 μg/mL NP_4-BSA or 5 μg/mL NP_{29}-BSA overnight at 4°C, washed and blocked with 2% BSA in PBS buffer (2 hours at 37°C), followed by addition of pre-diluted mice serum or culture supernatant and incubation at 37°C for 1 hour. After washing with 1xPBS, the captured antibodies were detected with 1:10,000 diluted HRP conjugated goat anti-mouse IgM, IgG, IgG1 and IgG2a secondary antibodies.

Real-time RT–PCR analysis

The total RNA was extracted with Trizol reagent (Invitrogen). Oligonucleotide (dT) and MMLV reverse transcriptase (Invitrogen) were used to prepare cDNA. The relative amount of cDNA was quantified by using the iQ SYBR real-time kit (Bio-Rad Laboratories) and normalized to β-actin. The realtime (RT)-PCR primers for Bcl6, Aicda, Blimp1, Cxcr5 and Cxcr4 were previously described (Liu et al., 2014), and the primers for Ascl2: forward, 5′-CGCTGCCCAGACTCATGCCC-3′; reverse, 5′-GCTTTACGCGGTTGCGCTCG-3′.

Retroviral transduction

Naive $CD19^+IgD^+CD38^-$ B cells isolated from Ascl2 ZsGreen or C57BL/6 mice were FACS sorted and activated with soluble LPS under neutral conditions for 24 hours, and were then infected with retroviruses Ascl2-RV-GFP, AID-RV-GFP, Id3-RV-GFP or control RV-GFP. One day after infection, the GFP+ cells were FACS sorted for various purposes as indicated.

KLH, NP-KLH and OVA-HEL immunization

The mice were immunized with 0.5 mg/ml of KLH, NP-KLH or OVA-HEL emulsified in CFA (1mg/ml) subcutaneously (100 μL per mouse) and were scarified and analyzed individually seven days later. The OVA-HEL conjugate was made with the HydraLink heterobifunctional conjugation kit (SoluLink) according to manufacturer's instructions. In brief, HEL was modified by 6-hydrazinonicotinamide and then allowed to react at a molar ration of 5:1 with OVA or BSA that was modified by 4-formylbenzoate. Excessive unconjugated HEL was then removed by size-exclusion chromatography. Germinal center B cells were analyzed by staining with FITC-labeled anti-FAS, APC-labeled anti-GL7, BV605-labeled anti-IgD and APCCy7-labeled anti-CD19 monoclonal antibody (BD PharMingen). Tfh cells were analyzed by staining with PE-Cy7-labeled anti-CD4 and botinylated anti-CXCR5 monoclonal antibodies, followed by APC-labeled streptavidin and surface staining by FITC-labeled anti-PD1 monoclonal antibody or intracellular staining by PE-CF594 labeled anti-Bcl6 monoclonal antibody (PharMingen). The serum was collected, and antigen-specific IgM, IgA, IgE, IgG1, IgG2a antibodies were measured by ELISA.

Flow Cytometry

The following fluorescent dye-conjugated anti-mouse antibodies were used for staining. For extracellular staining was performed using anti-CD4 (GK1.5; eBioscience), anti-CD44(IM7; Biolegend), anti-CD19 (1D3, BD Bioscience), anti-PD-1 (J43; BD Bioscience), anti-Fas (15A7; eBioscience), anti-GL7 (GL-7; eBioscience), biotinylated anti-CXCR5 (BD Bioscience) and Streptavidin (BD Bioscience); for intracellular staining was performed using anti-BCL6 (K112-92, BD Bioscience). Cells were analyzed on a LSRFortessa (BD) flow cytometer, and data analyzed using FlowJo IV. Dead cells were excluded based on viability dye staining (Fixable viability dye eF506, eBioscience).

Immunofluorescence staining

The immunofluorescence staining was performed as described previously (reference). Staining reagents included biotinylated PNA (Vector), AlexaFluor 488 anti-B220, and streptavidin AlexaFluor 594 (BD PharMingen). All stained slides were mounted with ProlongGold antifade reagents (Invitrogen) and examined with an Olympus LSM 780 confocal system.

Immunoglobulin sequence analysis

The intronic sequence of the 3′ to J_H4 exon of Igh gene was PCR amplified from genomic DNA of GC B cells using Phusion HF (Thermo) DNA polymerase and oligonucleotide primes as described previously (Gitlin et al., 2014). The PCR products were gel extracted, cloned into a pCR2.1-TOPO vector (Life Technologies), and sequenced, and aligned to the mm9 assembly of the mouse genomic sequence. The mutation frequencies in the J_H4 intronic region were calculated by dividing the total number of mutations from all clones with the total number of base pairs analyzed for each group.

Influenza virus infection

The influenza virus A/Puerto Rico/8 (PR8, H1N1) was obtained from Dr. Tang's lab, and were used to infect mice by intranasal administration at half of the LD_{50} dose as pre-tested. The mice were monitored daily, and the weight loss was recorded. To analyze influenza-virus-specific germinal center responses, The Tfh and germinal center B cells obtained from the lung mediastinal lymph nodes and spleens were analyzed by flow cytometry. The BALF and sera were collected 8 days post infection Virus-specific IgG antibodies were captured by heat-inactivated virus coated plate and analyzed by ELISA. The lung viral titers were monitored by examining influenza virus HA and neuraminidase (NA) gene expression using real-time RT-PCR as previously described (reference).

High-throughput sequencing and ChIP-seq

Total cellular RNA was extracted from cells transduced with vector or Ascl2-expressing retrovirus with TRIzol (Invitrogen). 30 million single-end 100 bp reads were sequenced per sample on the HiSeq2000/2500 V3 instrument (Illumina). DESeq analysis was used to identify differentially expressed genes and determine fold expression changes between groups.

The ASCL2 ChIP-seq was performed as described previously (Liu et al., 2014). Briefly, sorted B cells were fixed by 1% paraformaldehyde, followed by digestion with Mnase cocktail (Active motif). The chromatin obtained from 5×10^6 cells was used for each ChIP experiment. The Anti-ASCL2 monoclonal antibody was purchased from Millipore (clone 7E2). The pull-down DNA fragments were blunt-end ligated with Solexa adaptors, and amplified for sequencing. The DNA fragments were sequenced with an Illumina 1G Analyzer at the Institute for System Biology. The output of the Solexa Analysis Pipeline was converted to browser-extensible data (BED) files, sequencing reads were mapped to the mouse genome mm10 by bowtie2. The uniquely mapped reads were used to call peak with MACS2 using an FDR cutoff 0.01. ChIPseeker was used for peak annotation. The ChIP data were viewed in the UCSC genome browser. For motif analysis, HOMER was used to find TF motifs (homer.salk.edu).

QUANTIFICATION AND STATISTICAL ANALYSIS

Statistics

The statistic assays were performed with unpaired two-tailed Student's t tests or two-way analysis of variance (ANOVA) as indicated by using Graphpad Prism 6, and the data were presented as mean ± SEM when indicated. * represents $p < 0.05$, ** represents $p < 0.01$, *** represents $p < 0.005$; n.s = not significant.